13
Triggers

A well-designed trigger is an essential ingredient for a successful particle physics experiment. The trigger must efficiently pass the events under study without permitting the data collection systems to become swamped with similar but uninteresting background events. Since the design of a trigger depends critically on the intent of the experiment and is strongly influenced by the choice of beam parameters, target, geometry, and so forth, it is impossible to give a prescription here on how to set up a trigger for any situation. Instead, we must content ourselves in this chapter with considering some general classes of trigger elements and with examining some specific examples in more detail. It should be mentioned that some experiments do not use a trigger. For example, neutrino experiments sometimes accept any event that occurs within a gate following the acceleration cycle.

13.1 General considerations

A trigger is an electronic signal indicating the occurrence of a desired temporal and spatial correlation in the detector signals. The desired correlation is determined by examining the physical process of interest in order to find some characteristic signature that distinguishes it from other processes that will occur simultaneously. Most triggers involve a time correlation of the form $B \cdot F$, where B is a suitably delayed signal indicating the presence of a beam particle and F is a signal indicating the proper signature in the final state. The time coincidence increases the probability that the particles all come from the same event.

Let us first consider the beam portion of the trigger. Figure 13.1 shows a typical fixed target beam line containing scintillation counters S_1, S_2, and A, threshold Cerenkov counters C_1 and C_2, and PWC P_1. Suppose the

Downloaded from https://www.cambridge.org/core. IP address: 13.201.136.108, on 21 Aug 2025 at 16:06:51, subject to the Cambridge Core terms of use, available at https://www.cambridge.org/core/terms. https://doi.org/10.1017/9781009290098.014

experiment requires a K^- beam of a certain momentum at the target. With suitable gases and pressures in C_1 and C_2, the signal $C_1 \cdot \overline{C}_2$ can be used to separate kaons from pions and protons in the beam. The small scintillation counters S_1 and S_2 require that the beam particles traverse the Cerenkov counters near the beam axis. The anticounter (or veto counter) A is a large scintillation counter with a hole approximately the target diameter in the center. The anticounter is placed directly before the target. The signal from this counter vetos any event accompanied by an off-axis (or halo) particle, which could confuse the downstream detectors. The scintillation counter BC is a small counter placed directly in the path of the beam. It can be used to veto events accompanied by a beam track. The PWC P_1 can be used to ensure that only one beam track is present within a certain time interval. A typical kaon beam signal then is

$$B = S_1 \cdot S_2 \cdot C_1 \cdot \overline{C}_2 \cdot (P_1 = 1) \cdot \overline{A} \cdot \overline{BC}$$

The B signal as defined here can be used for devices that require a pretrigger. It is sometimes useful to record events with just the B requirement. This will give events with a minimum amount of bias with respect to the final state of interest. It is also useful for checking the efficiency of downstream detectors.

In a colliding beam machine a beam signal is usually provided each beam–beam crossing. This may result from the coincidence between two scintillator hodoscopes located close to the beam pipes or from pickup electrodes near the interaction point.

The final state portion of the trigger is obviously much more varied since it depends on the particular experiment. The F trigger usually makes use of some aspect of the topology of the desired events. These may include [1]

1. multiplicity,
2. direction,

Figure 13.1 A simple experimental arrangement of detectors. S_1, S_2, S_3, A, BC, CS: scintillation counters; C_1, C_2: threshold Cerenkov counters; P_1, P_2: MWPCs.

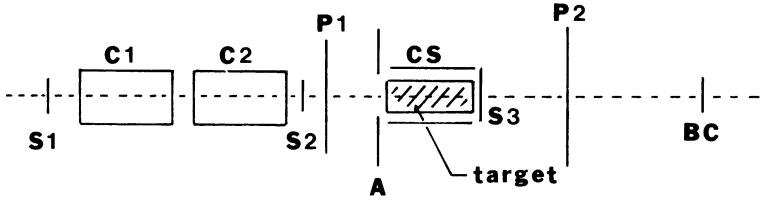

Downloaded from https://www.cambridge.org/core. IP address: 13.201.136.108, on 21 Aug 2025 at 16:06:51, subject to the Cambridge Core terms of use, available at https://www.cambridge.org/core/terms. https://doi.org/10.1017/9781009290098.014

3. deflection,
4. opening angle, and
5. coplanarity.

Multiplicity is frequently used in conjunction with other requirements. Here one demands that a certain number of particles are present at a specified location. Multiplicity is usually determined using a scintillator hodoscope or a MWPC. The multiplicity can also be used to set an upper limit to the number of particles in order to reject unanalyzable "junk" events.

Triggers frequently use a counter telescope or a hodoscope coincidence matrix to require that a particle points back to the target or interaction region. Two separate direction requirements may be combined to demand that a particle undergo a certain deflection or that a particle be produced at a given angle.

Particle kinematics can play an important role in the design of a trigger for reactions involving 2-body final states. This is particularly useful in elastic scattering. The final state particles and the beam must all lie in a plane (coplanarity). In addition, the beam momentum and forward scattering angle determine the forward and recoil momenta and the recoil scattering angle. In high rate reactions one can define narrow solid angles around these directions and require a coincidence between the signals from the two arms. An alternate approach is to use large solid angle detectors, but to use hodoscopes or hard-wired electronics to require the proper correlation.

Figure 13.2 shows the fast electronics for the 150-GeV/c pp elastic scattering experiment of Fidecaro et al. [2]. The INTERACTION coincidence indicates that there was one and only one particle in the forward (F) arm and at least one backward (B) particle in the counters around the target. The trigger also requires one and only one particle in the backward vertical (BV) and backward horizontal (BH) hodoscopes. The correlation between scattering angle and recoil energy is imposed by delaying the FV signal for a time corresponding to the recoil proton time of flight and then forming the coincidence WINDOW. A rough angular correlation between the backward and forward particles is made with the vertical coincidence matrix. Figure 13.3a shows the deviation of the measured forward proton angle in pp elastic scattering from the angle calculated from the recoil particle direction. Figure 13.3b shows the corresponding coplanarity distribution. The narrow distributions show that the trigger was very successful in selecting elastic events.

For the purpose of illustration let us consider a simple example. Sup-

Downloaded from https://www.cambridge.org/core. IP address: 13.201.136.108, on 21 Aug 2025 at 16:06:51, subject to the Cambridge Core terms of use, available at https://www.cambridge.org/core/terms. https://doi.org/10.1017/9781009290098.014

pose we are examining the reaction

$$K^- p \rightarrow \overline{K}^0 n$$

We have already discussed a suitable signal to tell us when a single K^- has come down the beam line. The target could be liquid hydrogen. The final state consists of two neutral particles, one of which will typically decay into two pions after a short distance. A signature in the detector that is indicative of a vee (decaying neutral particle) is no tracks followed some distance away by two tracks, or $0 \rightarrow 2$ for short. Thus, referring to Fig. 13.1, one could look for a forwardly produced $\overline{K}^0$ with the signal $\overline{S}_3 \cdot (P_2 = 2)$. Since the recoil neutron is also neutral, one could attempt to tighten the trigger by also vetoing with the cylindrical hodoscope CS surrounding the target. Thus, a suitable final state signal might be

$$F = \overline{S}_3 \cdot (P_2 = 2) \cdot \overline{CS}$$

Several factors complicate the design of a trigger. The first is the presence

Figure 13.2 Trigger logic for a pp elastic scattering experiment. Inputs are from horizontal (H) and vertical (V) scintillator hodoscopes in the forward (F) and backward (B) spectrometer arms and counters near the target. (G. Fidecaro et al., Nuc. Phys. B 173: 513, 1980.)

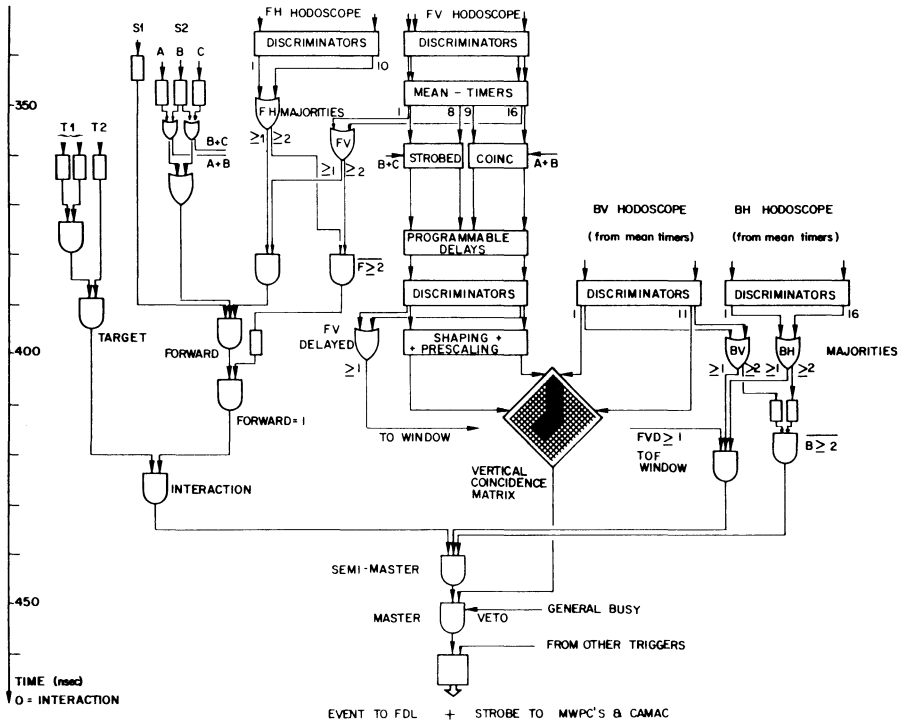

Downloaded from https://www.cambridge.org/core. IP address: 13.201.136.108, on 21 Aug 2025 at 16:06:51, subject to the Cambridge Core terms of use, available at https://www.cambridge.org/core/terms. https://doi.org/10.1017/9781009290098.014

of background reactions, which have similar characteristics to the process under study. In our example $\Lambda\pi^0$ is also an all neutral final state produced in K^-p interactions. The F signal will also be generated by this final state when the Λ is produced forwardly. If the background is significant, one must take further steps, such as surrounding the target with a thin lead cylinder to convert the photons from the π^0 decay.

A second problem is the presence of accidental hits in the detectors. These extra hits could arise from uncorrelated particles traversing the detector or from noise in the detector itself. Accidentals increase the number of hits in a detector and could give false F signals. A competing problem is chamber inefficiency. In this case there would be no hit in a detector plane, even though a charged particle crossed it. This leads to a loss of true F signals.

13.2 Identified particle triggers

Often we wish to trigger on the production of a certain type of particle. In this section we will consider the particles commonly used for

Figure 13.3 (a) Polar angle correlation between the measured angle for forwardly scattered particles and the forward angle calculated from the recoil particle direction for pp elastic scattering. (b) Measurement of the coplanarity of the beam, forward particle, and recoil particle. (G. Fidecaro et al., Nuc. Phys. B 173: 513, 1980.)

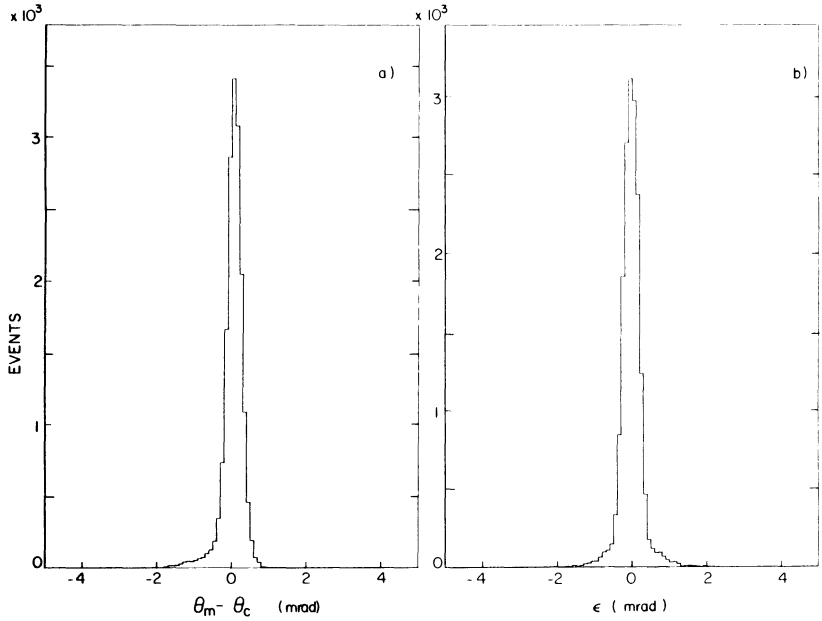

Downloaded from https://www.cambridge.org/core. IP address: 13.201.136.108, on 21 Aug 2025 at 16:06:51, subject to the Cambridge Core terms of use, available at https://www.cambridge.org/core/terms. https://doi.org/10.1017/9781009290098.014

Table 13.1. *Identified particle triggers*

Particle	Method	Example references
γ, π^0	multiplicity	G. Donaldson et al., Phys. Rev D 14: 2839, 1976
	lead-glass	R. Kephart et al., Phys. Rev D 14: 2909, 1976
	NaI	L. O'Neill et al., Phys. Rev D 14: 2878, 1976
	lead-scintillator	R. Baker et al., Nuc. Phys. B 156: 93, 1979
	liquid argon	D. Scharre et al., Phys. Rev D 23: 43, 1981
e	Cerenkov	A. Maki et al., Phys. Lett. 106B: 423, 1981
	lead-scintillator	D. Blockus et al., Nuc. Phys. B 201: 205, 1982
	transition radiator	M. Adams et al., Phys. Rev. D 27: 1977, 1983
	liquid argon	C. Kourkoumelis et al., Phys. Lett. 81B: 405, 1979
μ	penetration	B. Gordon et al., Phys. Rev. D 20: 2645, 1979
	magnetized iron	D. Antreasyan et al., Phys. Rev. Lett 45: 863, 1980
$\pi^{\pm}$	multiplicity	D. Aston et al., Nuc. Phys. B 166: 1, 1980
	Cerenkov	A. Berglund et al., Nuc. Phys. B 166: 25, 1980
$K^{\pm}$	Cerenkov	T. Armstrong et al., Nuc. Phys. B 224: 193, 1983
	K^+ detector	C.M. Jenkins et al., Phys. Rev. Lett. 51: 951, 1983
K^0	$n \rightarrow n+2$	C. Bromberg et al., Phys. Rev. D 22: 1513, 1980
	Cerenkov (π)	J. Wise et al., Phys. Lett. 98B: 123, 1981
	charged particle veto	M. Alston-Garnjost et al., Phys. Rev. D 17: 2226, 1978
$p, \bar{p}$ (fast)	Cerenkov	S.U. Chung et al., Phys. Rev. Lett. 45: 1611, 1980
p (recoil)	multiplicity	C. Daum et al., Nuc. Phys. B 182: 269, 1981
	range	K. Fujii et al., Nuc. Phys. B 187: 53, 1981
	solid state detector	R. Schamberger et al., Phys. Rev. D 17: 1268, 1978
$n, \bar{n}$	plastic scintillator	A. Robertson et al., Phys. Lett. 91B: 465, 1980
	liquid scintillator	R. Baker et al., Nuc. Phys. B 156: 93, 1979
	^{3}He-filled PWC	E. Pasierb et al., Phys. Rev. Lett. 43: 96, 1979

Downloaded from https://www.cambridge.org/core. IP address: 13.201.136.108, on 21 Aug 2025 at 16:06:51, subject to the Cambridge Core terms of use, available at https://www.cambridge.org/core/terms. https://doi.org/10.1017/9781009290098.014

Table 13.1. *(cont.)*

Particle	Method	Example references
	np elastic	K. Egawa et al., Nuc. Phys. B 188: 11, 1981
	charged particle veto	D. Cutts et al., Phys. Rev. D17: 16, 1978
$\Lambda\bar{\Lambda}$	$n \rightarrow n+2$	F. Lomanno et al., Phys. Lett. 96B: 223, 1980
	multiplicity	D. Aston et al., Nuc. Phys. B195: 189, 1982
	fast p	J. Bensinger et al., Phys. Rev. Lett. 50: 313, 1983

triggering and examine the techniques that have been used for their detection. Many of these subtriggers would not make a sufficiently tight trigger themselves but would be satisfactory if used in coincidence with other requirements on the interaction under study. Additional information such as time of flight or pulse heights may be recorded with every event. This can be used in the offline analysis to enhance the fraction of events containing rarer particles, such as K mesons or antiprotons. Table 13.1 contains a summary of identified particle techniques together with example references.

13.2.1 γ, π^0

Photons are usually identified by the large electromagnetic shower they create in matter. Lead sheets can be used to convert the photons. Methods used in detecting the photon include using multiplicity, lead–glass Cerenkov counters, NaI scintillation counters, lead–scintillation shower counters, and liquid argon calorimeters. One can distinguish showers created by electrons by using a thin scintillator veto before the photon detector. Additional scintillator requirements may be needed in the trigger to reduce background.

Triggers requiring a π^0 almost invariably make use of its 2γ decay mode. If the detector is sufficiently fine grained so that the two photons can be resolved, the π^0 events can be separated on the basis of the 2γ effective mass.

The production of "direct" photons is a subject of considerable interest [3]. By direct we mean photons that originate from the fundamental interactions of the hadronic constituents, as opposed to "ordinary" photons, which result from the electromagnetic decays of π^0's or other particles. This type of process is usually studied at large transverse momentum,

Downloaded from https://www.cambridge.org/core. IP address: 13.201.136.108, on 21 Aug 2025 at 16:06:51, subject to the Cambridge Core terms of use, available at https://www.cambridge.org/core/terms. https://doi.org/10.1017/9781009290098.014

so that the direct photon yield is enhanced. The π^0 decays can fake a direct photon event if either of the decay γ's is not detected or if the two decay γ's cannot be resolved by the detector. Thus, an experiment that attempts to directly measure the π^0 background requires a large solid angle, highly segmented γ detector.

A second method using thin convertors can be used to separate the classes of events [3]. The shower initiated by an unresolved π^0 is due to two γ's, while the shower from a direct γ event is only due to one. Thus, the conversion efficiencies are different, and the two types of events may be separated statistically. This method requires that any nonlinearities in the detector must be well understood. Both methods require good detection efficiency for low energy γ's in order to resolve asymmetric π^0 decays.

Figure 13.4 (a) Pulse height spectrum for e^+ triggers using an electromagnetic shower counter. The solid line events have an associated Cerenkov counter signal. (b) Pulse height spectrum from the shower counters for events without a Cerenkov counter signal. (c) Measured hadron contamination versus trigger transverse momentum. (D. Drijard et al., Phys. Lett. 108B: 361, 1982.)

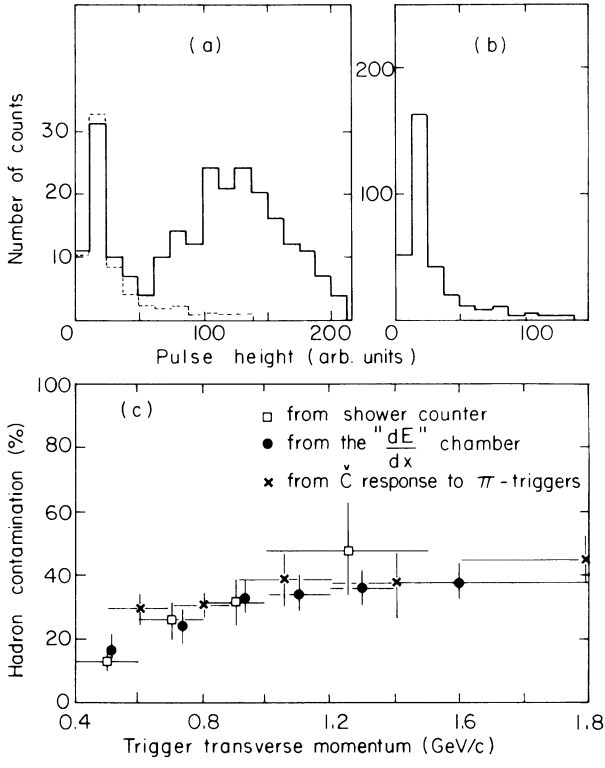

Downloaded from https://www.cambridge.org/core. IP address: 13.201.136.108, on 21 Aug 2025 at 16:06:51, subject to the Cambridge Core terms of use, available at https://www.cambridge.org/core/terms. https://doi.org/10.1017/9781009290098.014

13.2.2 e

Electrons and positrons are usually detected by the energy deposited by their electromagnetic shower. In certain momentum intervals a trigger may also be constructed using Cerenkov counters. Specific detection methods include using threshold Cerenkov counters, lead-scintillator shower counters, transition radiators, and liquid argon calorimeters. Major backgrounds include high momentum pions for Cerenkov counters and $e^+ e^-$ pairs from photon conversions. Figure 13.4 shows the pulse height spectrum for e^+ triggers from an electromagnetic shower counter [4]. The full-line spectrum in (a) is for triggers with an associated Cerenkov counter signal. The normalized dashed-line spectrum is for triggers with no Cerenkov signal. It is evident that the majority of low pulse height events are due to hadronic background. The Cerenkov and shower counter signals may be combined to produce a more efficient trigger.

13.2.3 μ

Muon triggers usually make use of the muons' ability to penetrate large depths of matter before being absorbed. Thus, the basic experimental arrangement would consist of a massive hadron absorber followed by a MWPC or counter hodoscope. Sometimes the functions of hadron absorber and spectrometer are combined by using magnetized iron toroids between the interaction point and the muon counters. The major background in the trigger comes from the small fraction of hadron "punch through" that manages to penetrate the absorber and from muons resulting from π and K decays.

A useful procedure for estimating the number of muons arising from hadron decays involves adjusting the amount of absorber [5]. By removing absorber, the probability that the hadron will decay is proportionally increased. This background rate is inversely proportional to the absorber density. By extrapolating the measured rate to infinite density, one can estimate the number of muon triggers not arising from hadron decays, as shown in Fig. 13.5.

13.2.4 $\pi^{\pm}$

Since pions are the most copiously produced hadrons, any arbitrary track in strong interactions is likely to be a pion. This is especially true in large multiplicity events ($n \geq 4$), which only have a small electromagnetic background. A tighter trigger could require pulses from a series of Cerenkov counters.

Downloaded from https://www.cambridge.org/core. IP address: 13.201.136.108, on 21 Aug 2025 at 16:06:51, subject to the Cambridge Core terms of use, available at https://www.cambridge.org/core/terms. https://doi.org/10.1017/9781009290098.014

13.2.5 $K^{\pm}$

The production rate of charged kaons is roughly 10% of the charged pion rate. Thus, filtering the kaons out of the pion background requires a fairly good trigger. Fast kaons can be selected using a pair of threshold Cerenkov counters. One counter is set to veto pions, while the second gives a positive kaon signal above a certain momentum. Triggers for slow K^+ recoils have been used with a K^- beam to study Ξ resonances. The trigger was derived from a K^+ detector similar to the one discussed in Section 12.6.

13.2.6 K^0

The trigger requirements for a K_S usually include the $n \rightarrow n + 2$ multiplicity requirement for a vee in some manner. The background, which includes Λ production and accidentals, can be cleaned up offline by cuts on the invariant mass of the decay tracks and the lifetime distribution. Sometimes the decay pions are required to give Cerenkov counter signals.

13.2.7 $p, \bar{p}$

Fast forward protons or antiprotons can be identified with large Cerenkov counters downstream of the interaction region. A recoil proton subtrigger is quite common as one part of an overall trigger requirement.

Figure 13.5 Muon event rate versus the inverse of the absorber density. Events have at least one muon with momentum greater than 8 GeV/c. (After J. Ritchie et al., Phys. Rev. Lett. 44: 230, 1980.)

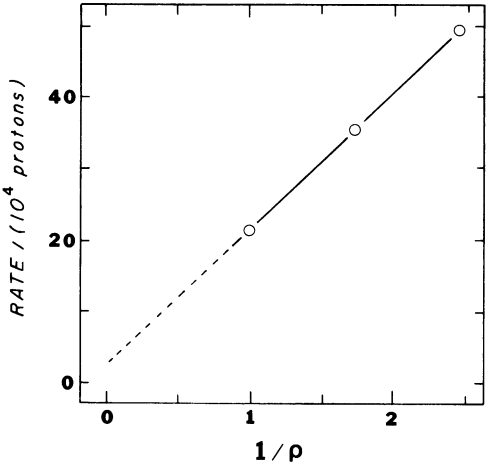

Downloaded from https://www.cambridge.org/core. IP address: 13.201.136.108, on 21 Aug 2025 at 16:06:51, subject to the Cambridge Core terms of use, available at https://www.cambridge.org/core/terms. https://doi.org/10.1017/9781009290098.014

The target can be surrounded by a scintillator hodoscope, and the trigger can make use of a multiplicity of one requirement. The exact requirement should be determined with care since a simple veto on more than one side counter firing could be biased because of delta ray production and interactions in the counters. For low momentum recoil protons a range absorber may be added with a counter behind the absorber used in anticoincidence.

13.2.8 $n, \bar{n}$

Neutron triggers make use of strong interactions of neutrons in matter. A recoil neutron subtrigger is common for interactions in deuterium, heavy nuclei, or in charge exchange scattering. Triggers have been constructed using plastic scintillator, liquid scintillator, ^{3}He filled gas PWC, and the recoil proton from np elastic scattering. When used with a thin veto counter to reject charged particles, the major backgrounds are from γ and K^0's.

13.2.9 $\Lambda, \overline{\Lambda}$

Most Λ triggers make use of the $p\pi^-$ decay mode. A common trigger uses the $n \rightarrow n + 2$ vee requirement. The $K^0 \rightarrow \pi^+\pi^-$ background can be suppressed by using a downstream Cerenkov counter in the area of acceptance of the decay proton. Simple multiplicity requirements on the downstream tracks may be sufficient to pick up Λ's. Analogous $\overline{\Lambda}$ triggers may be devised using its $\bar{p}\pi^+$ decay mode.

The decay proton emerges with most of the Λ momentum. We can give a rough kinematic argument why this is so. The Q (break up energy) for the Λ decay is small, so that in the Λ rest frame the π^- and p have only small momentum. In the Lorentz transformation to the laboratory frame the Λ acquires a velocity β. Since the π^- and p had only a small momentum in the Λ rest frame, they will also acquire a velocity $\approx \beta$ in the transformation to the LAB coordinate system. Thus, in the LAB

$$p_p = m_p\beta\gamma \qquad p_\pi = m_\pi\beta\gamma$$

so that the proton track tends to be much stiffer. The detection of a fast forward proton can be used to construct an efficient Λ trigger with π^- and K^- beams.

13.2.10 $\Sigma, \Xi, \Omega,$

The Σ, Ξ, and Ω hyperons can be used for triggering, particularly at high energies. We have already mentioned in Chapter 4 how DISC Cerenkov counters may be used to identify charged hyperons. The characteristic

Downloaded from https://www.cambridge.org/core. IP address: 13.201.136.108, on 21 Aug 2025 at 16:06:51, subject to the Cambridge Core terms of use, available at https://www.cambridge.org/core/terms. https://doi.org/10.1017/9781009290098.014

decay modes of the hyperons have also been used to construct triggers. We will consider these triggers in more detail since they consist of combinations of subtriggers for previously mentioned particles.

Wilkinson et al. [6] constructed a trigger for Σ^+ hyperons from the decay chain

$$\Sigma^+ \rightarrow p\pi^0 \qquad \pi^0 \rightarrow \gamma\gamma$$

They required a positively charged particle in the forward direction plus a minimum energy deposited in a lead–glass counter array. Approximately 6% of the triggers gave a reconstructed Σ^+. The signal was very clean. The major sources of background were accidental coincidences of beam tracks with γ's (3%) and $K^+ \rightarrow \pi^+\pi^0$ decays (2%).

A trigger for Σ^- was constructed from the decay mode [7]

$$\Sigma^- \rightarrow n\pi^-$$

The neutron was detected using a 2-absorption length steel–scintillator calorimeter. The front of the calorimeter was covered by a charged particle veto and 10 cm of lead–glass to veto photons. The trigger required a neutron signal in coincidence with a negative particle in the MWPCs. The trigger rate was 150 Σ^- triggers in the 800-ms beam spill per 5×10^8 protons incident on the production target.

Negative Ξ hyperons have been detected using a trigger based on the decay mode [8]

$$\Xi^- \rightarrow \Lambda\pi^- \qquad \Lambda \rightarrow \pi^- p$$

The trigger required a single charged particle before the decay region and at least one particle in both the right and left parts of a MWPC which followed the decay region and a bending magnet. The Ξ^- trigger was enhanced by requiring a stiff positive particle.

Cox et al. [9] have constructed a trigger for Ξ^0 using the decay chain

$$\Xi^0 \rightarrow \Lambda\pi^0 \qquad \pi^0 \rightarrow \gamma\gamma \qquad \Lambda \rightarrow \pi^- p$$

A neutral beam was defined using collimators, a sweeping magnet, and a scintillator veto. The Λ portion of the trigger required charged tracks in the positive and negative regions of a set of chambers following a bending magnet. Approximately 50% of the raw triggers contained a Λ. The photons from the π^0 decay were detected in either a lead-glass counter array or in a lead-scintillator shower detector. The Ξ^0/Λ ratio was 2%.

The lifetime of the Ω^- was measured by Bourquin et al. [10] using the CERN SPS charged hyperon beam. The beam was passed through a DISC Cerenkov counter. They triggered on the

$$\Omega^- \rightarrow \Lambda K^- \qquad \Lambda \rightarrow \pi^- p$$

Downloaded from https://www.cambridge.org/core. IP address: 13.201.136.108, on 21 Aug 2025 at 16:06:51, subject to the Cambridge Core terms of use, available at https://www.cambridge.org/core/terms. https://doi.org/10.1017/9781009290098.014

decay mode by requiring a coincidence between the DISC counter, a multiplicity counter ($n > 1$), and a small downstream (proton) counter that was inaccessible to negative particles. The trigger rate was 22 events per 10^6 beam particles. About 1% of the raw triggers contained an Ω^-. Backgrounds were mainly due to multiparticle events and Ξ^- decays. This experiment is discussed in more detail in Chapter 15.

13.3 Deposited energy triggers

Photons, electrons, π^0's, and jets are typically detected with a calorimeter. The simplest requirement for a trigger is that the total deposited energy in the detector exceed some threshold. With finely divided calorimeters one can sharpen the trigger by looking at the energy deposited in individual channels or clusters of channels or by looking at correlations between channels. Subdivision of the calorimeter elements gives the freedom to optimize the acceptance of the desired type of particle, while rejecting other types of particles or particles not originating from the region of interaction.

We will now consider several examples of this type of trigger. Amaldi et al. [11] used an array of lead-glass Cerenkov counters to trigger on single photons at the ISR. The counters were arranged in a 9×15 matrix and mounted on rails so that the distance to the beam intersection point could be adjusted. Several triggers were used. In the first the counters were divided into fifteen 3×3 submatrices, and the nine counters in each submatrix were connected in parallel. A trigger was generated when at least one of the submatrices showed a deposited energy greater than the electronic threshold of 1.25 GeV. A second trigger required that one of the 5×3 central counters show a deposited energy greater than an electronic threshold of 0.5 GeV. The major backgrounds for the direct photon search were signals from π^0 or η, where one of the decay photons was not detected or was unresolved, and from the annihilation of $\bar{n}$ in the lead-glass producing additional π^0's.

Gollin et al. [12] used a calorimeter as part of a two-muon trigger at Fermilab. The calorimeter was constructed from 15 modules, each consisting of five alternating layers of steel plates and scintillation counters. The steel plates were magnetized and served as targets for the beam muons. The counters in consecutive modules were grouped into overlapping clusters of 10. The trigger required that at least 5 of the 10 counters in any cluster exceed some threshold. This requirement selected hadrons preferentially, since electromagnetic showers have a shorter longitudinal development. The trigger efficiency curve was quite broad, rising from 10 to 90% over about 50GeV in shower energy.

Downloaded from https://www.cambridge.org/core. IP address: 13.201.136.108, on 21 Aug 2025 at 16:06:51, subject to the Cambridge Core terms of use, available at https://www.cambridge.org/core/terms. https://doi.org/10.1017/9781009290098.014

Cobb et al. [13] used a finely divided liquid argon calorimeter at the ISR to trigger on the production of single particles and jets with large transverse momentum. The trigger required a total energy deposit above threshold in the calorimeter. This requirement is not sufficient to efficiently trigger on large p_t single particles, since it is also satisfied by events with a large number of low energy particles. For this reason, they also imposed a localized energy deposit requirement on the trigger. Overlapping clusters of four or five calorimeter elements were summed together in each coordinate and the sums were taken in coincidence.

Bromberg et al. [14] also used a calorimeter to provide a trigger signal proportional to the transverse momentum of single particles or jets. The experiment had four calorimeter modules on each side of the beam. Each calorimeter module had an electromagnetic front end consisting of lead and steel sheets interleaved with plastic scintillators. This was followed by a hadronic section consisting of alternating iron and scintillator layers. The scintillator signals in the electromagnetic section of each module were summed together, as were the hadronic signals. The signals from the four PMTs associated with each module were summed together and attenuated appropriately so that the resulting signal was proportional to the transverse momentum. The single particle trigger required that the signal in one of the eight modules exceed some threshold. For the jet trigger the signals from the four modules on each side of the beam were combined and the sum required to exceed a threshold. Figure 13.6 shows the transverse momentum distribution of jet-triggered events for two different threshold conditions. The plotted p_t value was calculated from ADC information from each of the PMTs. The ADC signal was proportional to the area under the pulse signal, while the trigger hardware was only sensitive to the height of the signal. For this reason, the distribution shown in Fig. 13.6 does not have a sharp threshold.

13.4 Higher level triggering

In some experiments involving rare processes, a second or third level of triggering is required after an event passes the fast triggers we have discussed up to now. The purpose of the high level triggers is to enrich the sample of recorded events or to increase the sensitivity of the experiment [15]. By rejecting noninteresting events at the trigger stage, the number of data tapes is reduced, thereby simplifying bookkeeping and handling and reducing the time necessary to analyze the data. In addition, if a decision regarding the noninteresting events can be made in a time shorter than the data readout time, the deadtime of the experiment can be reduced and the

Downloaded from https://www.cambridge.org/core. IP address: 13.201.136.108, on 21 Aug 2025 at 16:06:51, subject to the Cambridge Core terms of use, available at https://www.cambridge.org/core/terms. https://doi.org/10.1017/9781009290098.014

sensitivity to interesting events can be increased. The higher level triggers can enrich the data sample by (1) eliminating events with insufficient information that will eventually be discarded by the offline analysis programs; (2) demanding the presence of at least one track with a specific charge, angle, or momentum; or (3) requiring the overall event to satisfy a specific kinematic constraint.

The trigger generally uses a programmable device such as (1) a look-up table, (2) a hard-wired processor, (3) a microprogrammable processor, or (4) an emulator [15]. A look-up table is generally a random-access memory (RAM), which is addressed by signals from the detectors of the experiment. The look-up table may be used in a logical mode, whereby the incoming detector signals form a bit pattern, which corresponds to an address in RAM. The addressed location need only contain a single bit specifying whether that bit pattern was acceptable or not. When used in an arithmetic mode, the address can be formed by an operand to evaluate the value of a function. Hard-wired processors can execute a particular

Figure 13.6 Transverse momentum distribution of triggered particles in a calorimeter. Data are shown for two values of the detector threshold. (After C. Bromberg et al., Nuc. Phys. B 171: 1, 1980.)

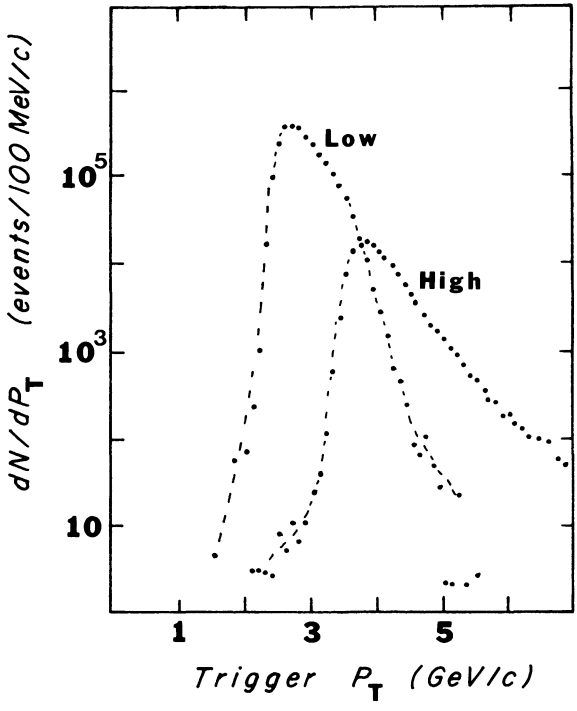

Downloaded from https://www.cambridge.org/core. IP address: 13.201.136.108, on 21 Aug 2025 at 16:06:51, subject to the Cambridge Core terms of use, available at https://www.cambridge.org/core/terms. https://doi.org/10.1017/9781009290098.014

algorithm very quickly, but it is difficult to change the algorithm on short notice. Greater flexibility is available in a microprogrammable processor. However, these devices must be programmed in microcode. Emulators are microprocessors that can execute the instruction set of a high level machine. They are the easiest of these devices to program but are also slower.

An example of eliminating events that will eventually be rejected is a "loose track requirement." Eventually an offline analysis program will be used to determine a particle track from the pattern of chamber hits (accidental or real) in the tracking chambers. The program will require some minimum number of hits along a path before it can reliably recognize a track. A typical drift chamber uses a double layer of drift cells with the layers offset by half a cell width to help resolve the left–right ambiguity. A microprocessor can be used to determine the number of these double planes that have hits in adjacent cells and to veto events that do not have a sufficient number.

A second category of higher level trigger selects events where at least one track has some property. Pizer et al. [16] have developed a programmable track selector (PTS) using a look-up memory table that can make track validity decisions in less than 1 μs. The system uses two MWPCs as inputs. Each of the 1024 wires in the first chamber addresses a word in memory. Each memory location contains the first and last wire numbers in the second chamber, which form a valid combination with that wire in the first chamber. This device can be used to make rough momentum selections or to test for angular or coplanarity correlations in elastic scattering. Fidecaro et al. [2] have used the PTS as part of a pp elastic scattering trigger. One PTS was used to demand a positive recoil particle coming from the target. A second PTS required a high momentum forwardly produced positive particle.

A similar device has been used at the Omega spectrometer at CERN to enhance the trigger fraction for K^+ production [17]. Three planes of scintillator hodoscopes and two Cerenkov counters were used as inputs to the programmable trigger. Because of the presence of a magnetic field, a correlation exists between the hits in any two planes for particles of a given charge and in a restricted momentum interval. Signals from some of the planes were used as inputs to an ECL RAM module called a bit assigner. For each input the bit assigner contained a pattern of bits that should be present for another hodoscope if the signals from the event satisfy the correlation. The output of the bit assigner was then sent to a unit that performed a bit by bit AND with the actual signals from the second plane.

Downloaded from https://www.cambridge.org/core. IP address: 13.201.136.108, on 21 Aug 2025 at 16:06:51, subject to the Cambridge Core terms of use, available at https://www.cambridge.org/core/terms. https://doi.org/10.1017/9781009290098.014

Two-input trigger matrices have been used for triggering the European Muon Spectrometer at CERN [18]. A simplified experimental layout and logic diagram for a single muon trigger are shown in Fig. 13.7. Horizontal and vertical scintillator hodoscope were used downstream of the bending magnet. The hodoscope information was input into two trigger matrices (M1 and M5) to determine if the track pointed back toward the target. The shaded areas on M1 and M5 in Fig. 13.7 represent coincidences corresponding to good tracks. The outputs of the target-pointing matrices were used as inputs to additional trigger matrices, which selected final state muons whose scattering angle (M2) and momentum (M3) were larger than preselected values. A NIM output was provided from the trigger matrix for those channels where the coincidence requirement was satisfied. The input–output delay for obtaining a good signal was only 25 ns. The matrix could be manually set or programmed using CAMAC.

If a third plane is added to the correlation requirement, the momentum

Figure 13.7 Trigger logic diagram for single muon events at the European Muon Spectrometer. (O. Allkofer et al., Nuc. Instr. Meth. 179: 445, 1981.)

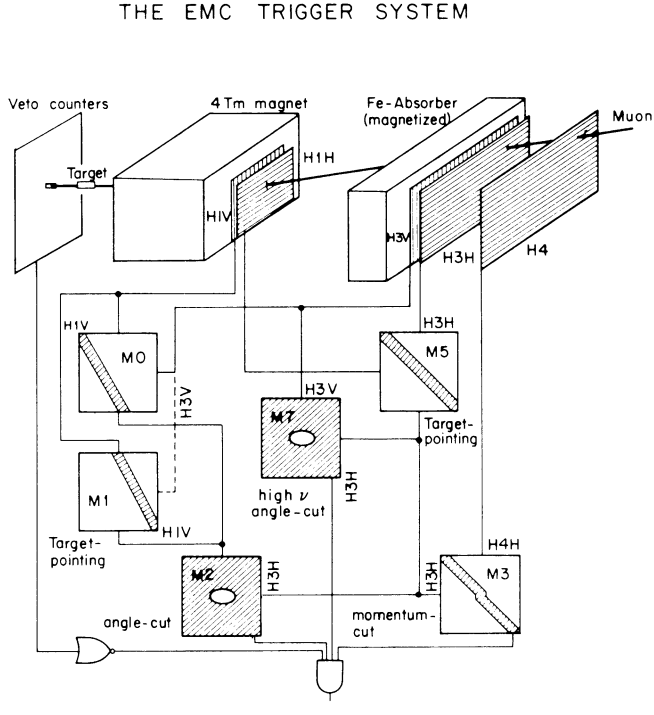

Downloaded from https://www.cambridge.org/core. IP address: 13.201.136.108, on 21 Aug 2025 at 16:06:51, subject to the Cambridge Core terms of use, available at https://www.cambridge.org/core/terms. https://doi.org/10.1017/9781009290098.014

of the particle can be tightly specified in addition to its charge. Such a device (RAM) has been built at the Multi Particle Spectrometer at BNL [19]. The RAM is a 3-dimensional array of programmable AND gates. Each dimension of the RAM has a corresponding fine-grained detector array as input. The detector output is strobed into a fast register and used to address a particular location in memory. The memory is loaded with a pattern of logical 0's and 1's before the experiment on the basis of Monte Carlo studies of the predicted behavior of the trigger particles. If a logical 1 is present in the addressed memory location, the RAM will pass a higher level trigger signal.

The RAM is a high resolution device that can determine if the 3-dimensional correlation is satisfied within 250 ns. It is easily adaptable to different experiments by simply reprogramming the pattern of 0's and 1's. The pattern can be checked during an experiment by comparing the memory pattern with a disc file between beam spills. The device responds accurately in the presence of additional particles. In addition, it can be used to demand the presence of more than one particle of the required type.

Lastly we will describe a mass dependent trigger used in a muon pair production experiment at Fermilab [20]. The experiment was designed to study the properties of short-lived, high mass states that decay into muon pairs. The effective mass of a state can be written

$$M^2 \approx 2p_1 p_2 (1 - \cos\theta) \tag{13.1}$$

when $p_1 \gg m_\mu$ and $p_2 \gg m_\mu$. Unfortunately, the production of low mass muon pairs exceeds by many orders of magnitude the production of the more interesting higher mass pairs. In order to improve the efficiency of data collection, the experimenters constructed a mass dependent trigger.

Figure 13.8 Detector arrangement for use with a two-muon effective mass trigger. (M) bending magnet; (J_x, J_y, F_x) scintillator hodoscopes. (After G. Hogan, Nuc. Instr. Meth. 165: 7, 1979.)

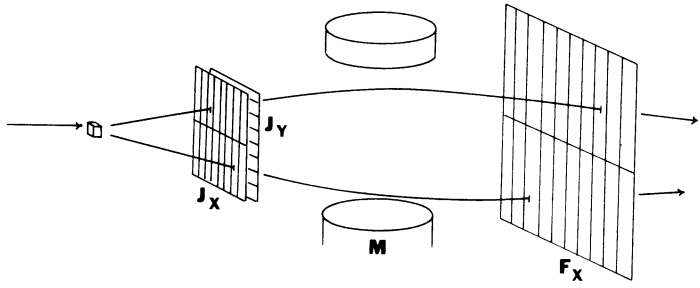

Downloaded from https://www.cambridge.org/core. IP address: 13.201.136.108, on 21 Aug 2025 at 16:06:51, subject to the Cambridge Core terms of use, available at https://www.cambridge.org/core/terms. https://doi.org/10.1017/9781009290098.014

Figure 13.8 shows a schematic of the experimental arrangement. There is a double layer hodoscope (J_x and J_y) between the target and the bending magnet and an x-measuring hodoscope after the magnet. The basic idea of the trigger is to use the correlations in the hodoscope planes to determine p_1, p_2, and θ and then to use a hard-wired digital processor to determine M. Consider the logarithm of Eq. 13.1,

$$\ln \tfrac{1}{2} M^2 = \ln p_1 + \ln p_2 + \ln(1 - \cos \theta) \tag{13.2}$$

If we assume the muons are produced in the target, the separation of the hits in J_x and J_y will determine the opening angle θ, and the positions of the two hits in J_x and F determine the momenta p_1 and p_2. The hodoscope signals were input into gate matrices constructed so that the output was $\ln p_1$, $\ln p_2$, and $\ln(1 - \cos \theta)$. These signals then entered a digital adder, which generated a signal that monotonically increased with muon pair mass. This signal was compared with a switch-selected, mass-cut value to determine whether or not to accept an event.

The trigger was able to select high mass muon pairs in less than 300 ns. The mass resolution is shown in Fig. 13.9. It can be seen that one can choose a mass cut to study the production of a high mass state such as the J/ψ and at the same time eliminate much of the background from low mass states, such as the ρ.

Figure 13.9 Accepted effective mass distribution using the mass dependent trigger. (After G. Hogan, Nuc. Instr. Meth. 165: 7, 1979.)

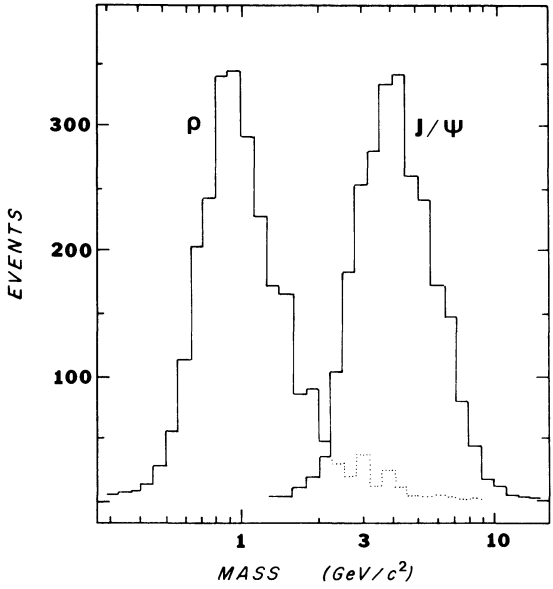

Downloaded from https://www.cambridge.org/core. IP address: 13.201.136.108, on 21 Aug 2025 at 16:06:51, subject to the Cambridge Core terms of use, available at https://www.cambridge.org/core/terms. https://doi.org/10.1017/9781009290098.014

References

The references given in this chapter should aid the reader in finding a more complete description of the hardware used in the triggers, rates, backgrounds, etc., and are of course a good source of additional references. Another excellent source of references concerning experiments with specified beams, final state particles, and momentum regions is the Particle Data Group, An indexed Compilation of Experimental High Energy Physics Literature, LBL-90, September 1978.

[1] M. Turala, Application of wire chambers for triggering purposes, Nuc. Instr. Meth. 176: 51–60, 1980.

[2] G. Fidecaro, M. Fidecaro, L. Lanceri, S. Nurushev, L. Piemontese, Ch. Poyer, V. Solovianov, A. Vascotto, F. Gasparini, A. Meneguzzo, M. Posocco, C. Voci, R. Birsa, F. Bradamante, M. Giorgi, A. Penzo, P. Schiavon, A. Villari, W. Bartl, R. Fruhwirth, Ch. Gottfried, G. Leder, W. Majerotto, G. Neuhofer, M. Pernicka, M. Regler, M. Steuer and H. Stradner, Measurement of the polarization parameter in pp elastic scattering at 150 GeV/*c*, Nuc. Phys. B173: 513–45, 1980.

[3] T. Ferbel and W. Molzon, Direct photon production in high energy collisions, Rev. Mod. Phys. 56: 181–221, 1984.

[4] D. Drijard, H.G. Fischer, H. Frehse, W. Geist, P.G. Innocenti, D.W. Lamsa, W. T. Meyer, A. Norton, O. Ullaland, H.D. Wahl, G. Fontaine, C. Ghesquiere, G. Sajot, W. Hofmann, M. Panter, K. Rauschnable, J. Spengler, D. Wegener, P. Hanke, M. Heiden, E.E. Kluge, T. Nakada, A. Putzer, M. Della Negra, D. Linglin, R. Gokieli, and R. Sosnowski, Further investigation of beauty baryon production at the ISR, Phys. Lett. 108B: 361–6, 1982.

[5] J. Ritchie, A. Bodek, R. Coleman, W. Marsh, S. Olsen, B. Barish, R. Messner, M. Shaevitz, E.Siskind, H. Fisk, Y. Fukushima, G. Donaldson, F. Merritt, and S. Wojcicki, Prompt muon production at small x_F and P_T in 350 GeV p-Fe collisions, Phys. Rev. Lett. 44: 230–3, 1980.

[6] C. Wilkinson, R. Handler, B. Lundberg, L. Pondrom, M. Sheaff, P. Cox, C. Dukes, J. Dworkin, O. Overseth, A. Beretvas, L. Deck, T. Devlin, K. Luk, R. Rameika, R. Whitman, and K. Heller, Polarization of Σ^+ hyperons produced by 400 GeV protons, Phys. Rev. Lett. 46: 803–6, 1981.

[7] L. Deck, A. Beretvas, T. Devlin, K. Luk, R. Rameika, R. Whitman, R. Handler, B. Lundberg, L. Pondrom, M. Sheaff, C. Wilkinson, P. Cox, C. Dukes, J. Dworkin, O. Overseth, and K. Heller, Polarization and magnetic moment of the Σ^- hyperon, Phys. Rev. D 28: 1–20, 1983.

[8] R. Handler, R. Grobel, B. Lundberg, L. Pondrom, M. Sheaff, C. Wilkinson, A. Beretvas, L. Deck, T. Devlin, B. Luk, R. Rameika, P. Cox, C. Dukes, J. Dworkin, O. Overseth, and K. Heller, Magnetic moments of charged hyperons, in G. Bunce (Ed.), *High Energy Spin Physics—1982,* AIP Conf. Proc. No. 95, New York: AIP, 1983, pp. 58–63.

[9] P. Cox, J. Dworkin, O. Overseth, R. Handler, R. Grobel, L. Pondrom, M. Sheaff, C. Wilkinson, L. Deck, T. Devlin, K. Luk, R. Rameika, P. Skubic, K. Heller, and G. Bunce, Precise measurement of the Ξ^0 magnetic moment, Phys. Rev. Lett. 46: 877–80, 1981.

[10] M. Bourquin, R.M. Brown, J. Chollet, A. Degre, D. Froidevaux, J. Gaillard, C. Gee, J. Gerber, W. Gibson, P. Igo-Kemenes, P. Jeffreys, M. Jung, B. Merkel, R. Morand, H. Plothow-Besch, J. Repellin, J. Riester, B. Saunders, G. Sauvage, B. Schiby, H. Siebert, V. Smith, K. Streit, R. Strub, J. Thresher, and S. Tovey, Measurement of Ω^- decay properties in the CERN SPS hyperon beam, Nuc. Phys. B241: 1–47, 1984.

[11] E. Amaldi, M. Beneventano, B. Borgia, A. Capone, F. DeNotaristefani, U. Dore, F.

Downloaded from https://www.cambridge.org/core. IP address: 13.201.136.108, on 21 Aug 2025 at 16:06:51, subject to the Cambridge Core terms of use, available at https://www.cambridge.org/core/terms. https://doi.org/10.1017/9781009290098.014

Ferroni, E. Longo, L. Luminari, P. Pistilli, I. Sestilli, G.F. Dell, L.C.L. Yuan, G. Kantardjian, and J. Dooher, Single direct photon production in pp collisions at $\sqrt{s} = 53.2$ GeV in the P_t interval 2.3 to 5.7 GeV/c, Nuc. Phys. B150: 326–44, 1979.

[12] G.D. Gollin, F.C. Shoemaker, P. Surko, A.R. Clark, K.J. Johnson, L.T. Kerth, S.C. Loken, T.W. Markiewicz, P.D. Meyers, W.H. Smith, M. Strovink, W.A. Wenzel, R.P. Johnson, C. Moore, M. Mugge, and R.E. Shafer, Charm production by muons and its role in scale non-invariance, Phys. Rev. D 24: 559–89, 1981.

[13] J. Cobb, S. Iwata, D. Rahm, P. Rehak, I. Stumer, C. Fabjan, M. Harris, J. Lindsay, I. Mannelli, K. Nakamura, A. Nappi, W. Struczinski, W. Willis, C. Kourkoumelis, and A. Lankford, A large liquid argon shower detector for an ISR experiment, Nuc. Instr. Meth. 158: 93–110, 1979.

[14] C. Bromberg, G. Fox, R. Gomez, J. Pine, J. Rohlf, S. Stampke, K. Yung, S. Erhan, E. Lorenz, M. Medinnis, P. Schlein, V. Ashford, H. Haggerty, R. Juhala, E. Malamud, S. Mori, R. Abrams, R. Delzenero, H. Goldberg, S. Margulies, D. McLeod, J. Solomon, R. Stanek, A. Dzierba, and W. Kropac, Jet production in high energy hadron-proton collisions, Nuc. Phys. B 171: 1–37, 1980.

[15] C. Verkerk, Use of intelligent devices in high energy physics experiments, in C. Verkerk (ed.), Proc. of the 1980 CERN School of Computing, CERN Report 81-03, pp. 282–324.

[16] I. Pizer, J. Lindsay, and G. Delavallade, Programmable track selector for nuclear physics experiments, Nuc. Inst. Meth. 156: 335–8, 1978.

[17] T. Armstrong, W. Beusch, A. Burns, I. Bloodworth, E. Calligarich, G. Cecchet, R.Dolfini, G. Liguori, L. Mandelli, M. Mazzanti, F. Navach, A. Palano, V. Picciarelli, L. Perini, Y. Pons, M. Worsell, and R. Zitoun, Using MBNIM electronics for the trigger in a high energy physics experiment, Nuc. Inst. Meth. 175: 543–7, 1980.

[18] O.C. Allkofer, J.J. Aubert, G. Bassompierre, K.H. Becks, Y. Bertsch, C. Besson, C. Best, E. Bohm, D.R. Botterill, F.W. Brasse, C. Broll, J. Carr, B. Charles, R.W. Clifft, J.H. Cobb, G. Coignet, F. Combley, J.M. Crespo, P.F. Dalpiaz, P. Dalpiaz, W.D. Dau, J.K. Davies, Y. Declais, R.W. Dobinson, J. Drees, A. Edwards, M. Edwards, J. Favier, M.I. Ferrero, J.H. Field, W. Flauger, E. Gabathuler, R. Gamet, J. Gayler, P. Ghez, C. Gossling, J. Haas, U. Hahn, K. Hamacher, P. Hayman, M. Henckes, H. Jokisch, J. Kadyk, V. Korbel, M. Maire, L. Massonnet, A. Melissinos, W. Mohr, H.E. Montgomery, K. Moser, R.P. Mount, M. Moynot, P.R. Norton, A.M. Osborne, P. Payre, C. Peroni, H. Pessard, U. Pietrzyk, K. Rith, M.D. Rousseau, E. Schlosser, M. Schneegans, T. Sloan, M. Sproston, W. Stockhausen, H.E. Stier, J.M. Thenard, J.C. Thompson, L. Urban, M. Vivargent, G. von Holtey, H. Wahlen, E. Watson, V.A. White, D. Williams, W.S.C. Williams and S.J. Wimpenny, A large magnetic spectrometer system for high energy muons, Nuc. Inst. Meth. 179: 445–66, 1981.

[19] E. Platner, A. Etkin, K. Foley, J.H. Goldman, W. Love, T. Morris, S. Ozaki, A. Saulys, C. Wheeler, E. Willen, S. Lindenbaum, J. Bensinger, and M. Kramer, Programmable combinational logic trigger system for high energy particle physics experiments, Nuc. Instr. Meth. 140: 549–52, 1977.

[20] G. Hogan, Design of a fast mass dependent trigger, Nuc. Instr. Meth. 165: 7–13, 1979.

Exercises

1. Design a subtrigger for a fixed target accelerator experiment that produces a signal OPEN whenever there are two downstream

Downloaded from https://www.cambridge.org/core. IP address: 13.201.136.108, on 21 Aug 2025 at 16:06:51, subject to the Cambridge Core terms of use, available at https://www.cambridge.org/core/terms. https://doi.org/10.1017/9781009290098.014

tracks with an opening angle greater than 1°. Include a description of the detectors, their arrangement, and electronics.

2. The dominant decay modes of the η meson are

$$\eta \rightarrow \gamma\gamma \quad (39\%) \rightarrow 3\pi^0 \quad (32\%)$$

Design a trigger to study the 2γ decay mode. What can you do to minimize the background from $3\pi^0$?

3. The charmed D^+ mesons have a $c\tau = 0.028$ cm and a significant branching ratio into a K^- plus pions. Design a trigger to study D^+ decays.

4. Show that the fraction F of potential events that can be recorded by a data acquisition system is

$$F = (1 + R\tau)^{-1}$$

where R is the trigger rate and τ is the time needed to read out an event. What trigger rate can be tolerated if the deadtime fraction should be less than 10% and if the readout time is 2 μs?

5. Define the sensitivity S of a trigger to be the rate at which good events are recorded. Show that the sensitivity of a two-level trigger is

$$S = \frac{pfR}{1 + R(t + f\tau)}$$

where p is the purity of the event sample selected by the second-level trigger, R is the first-level trigger rate, t is the second-level decision time, f is the fraction of events that pass the second-level trigger, and τ is the readout time. Examine the quantities in this equation to determine under what conditions a two-level trigger can make a significant improvement in sensitivity.

6. Suppose that a calorimeter experiment defines a good trigger event to be any one in which the sum (p_t) of the magnitudes of the deposited transverse momenta equals or exceeds a threshold value (q). Assume that the probability of getting an event with transverse momentum p is $\propto \exp(-\beta p)$ and that the calorimeter can only resolve p_t to within $\pm\delta p_t$, where $0 \leqslant \delta \leqslant 1$. Show that the ratio r of the probability of getting a trigger in which the actual p_t is less than q to the probability of a good trigger is

$$r = \exp(\delta\beta q) - 1$$

Downloaded from https://www.cambridge.org/core. IP address: 13.201.136.108, on 21 Aug 2025 at 16:06:51, subject to the Cambridge Core terms of use, available at https://www.cambridge.org/core/terms. https://doi.org/10.1017/9781009290098.014